Shell-Cross-Linked Micelles Containing Cationic Polymers Synthesized via the RAFT Process: Toward a More Biocompatible Gene Delivery System

Ling Zhang, T. L. Uyen Nguyen, Julien Bernard,† Thomas P. Davis, Christopher Barner-Kowollik, and Martina H. Stenzel*

Centre for Advanced Macromolecular Design (CAMD), School of Chemical Sciences and Engineering, The University of New South Wales, Sydney, NSW 2052, Australia

Received April 3, 2007; Revised Manuscript Received June 18, 2007

Block copolymers poly(2-(dimethylamino) ethyl methacrylate)-*b*-poly(polyethylene glycol methacrylate) (PDMAEMA-*b*-P(PEGMA)) were prepared via reversible addition fragmentation chain transfer polymerization (RAFT). The polymerization was found to proceed with the expected living behavior resulting in block copolymers with varying block sizes of low polydispersity (PDI <1.3). The resulting block copolymer was self-assembled in an aqueous environment, leading to the formation of pH-responsive micelles. Further stabilization of the micellar system was performed in water using ethylene glycol dimethacrylate and the RAFT process to cross-link the shell. The cross-linked micelle was found to have properties significantly different from those of the uncross-linked block copolymer micelle. While a distinct critical micelle concentration (CMC) was observed using block copolymers, the CMC was absent in the cross-linked system. In addition, a better stability against disintegration was observed when altering the ionic strength such as the absence of changes of the hydrodynamic diameter with increasing NaCl concentration. Both cross-linked and uncross-linked micelles displayed good binding ability for genes. However, the cross-linked system exhibited a slightly superior tendency to bind oligonucleotides. Cytotoxicity tests confirmed a significant improvement of the biocompatibility of the synthesized cross-linked micelle compared to that of the highly toxic PDMAEMA. The cross-linked micelles were taken up by cells without causing any signs of cell damage, while the PDMAEMA homopolymer clearly led to cell death.

Introduction

Oligonucleotides (ONs) are short single strands of DNA, containing 10−30 nucleotides. Synthetic antisense oligonucleotides (ASONs), also called magic bullets, are promising as clinical therapeutic regimen for genetic, neoplastic, and infectious diseases,[1−3] such as human immunodeficiency virus (HIV), hypertension, cardiovascular disease, and leukemia.[4] ASONs have the ability to specifically inhibit mutated genes or foreign genes and to permanently replace a missing or deficient gene.[1] One major advantage of ASON therapy over conventional treatments is that synthetic ASONs show a high degree of specificity to these diseases and do not elicit an immune response.[3]

However, several major obstacles still limit the successful delivery of ASONs. ASONs can easily be damaged by nucleases, which are ubiquitous in the body. Furthermore, equivalent to conventional drugs, the ultimate goal of drug treatment is the targeted delivery to a specific site. For ASONs to convey their full potential, they are required to find particular targets[4] in the human body.

To date, various methods have been studied, for example, chemical modifications, using viral or non-viral systems. At least three generations of chemically modified ASONs based on phosphorothioate DNA have been investigated.[5−8] Chemical modification of ASONs could largely increase the half-life of ASONs in plasma; however, phosphorothioate ASONs could then bind to certain proteins, causing cellular toxicity.[9]

Currently, viral systems are widely used as gene delivery vectors because of their ability to efficiently promote DNA delivery and DNA expression.[10] However, virus-based vectors as gene delivery systems can introduce high risks in toxicity and immunogenicity. Furthermore, the technique is usually not cost-efficient.

Polymeric gene delivery systems have been widely explored as a viable alternative to viral systems.[11] Polycationic polymers, such as polyethylenimine, poly-L-lysine and polymethacrylate/methacrylamide have been largely used because of their ability to condense DNA for more efficient uptake.[10] Poly(2-dimethylaminoethyl methacrylate) (PDMAEMA) is now widely utilized and extensively studied as a gene/drug delivery system.[12−14] In addition, PDMAEMA shows other interesting characteristics such as pH sensitivity,[15] a very attractive property in biomedical applications.[16−21] However, the use of cationic polymers is partly hampered because of their toxicity. Several efforts have been undertaken to reduce toxicity while maintaining high transfection efficiency.[22]

Amphiphilic copolymers can be considered as suitable gene/drug delivery carriers.[23] In a physiological environment, amphiphilic copolymers form aggregates such as micelles, vesicles, or rods with the hydrophobic blocks as the core and hydrophilic blocks as the shell. Drugs are usually encapsulated in the hydrophobic compartment, while the hydrophilic corona ensures the protection of the complex and increases its solubility and mobility. The shell-forming polymer is in addition responsible for the biocompatibility of the system.

High degree of biocompatibility and ease of modification are attractive features of poly(ethylene glycol) (PEG)-based poly-

* Corresponding author. E-mail: camd@unsw.edu.au or M.Stenzel@unsw.edu.au.

† Current address: CNRS, LMM/IMP INSA LYON, France.

10.1021/bm070370g CCC: $37.00
Published on Web 08/11/2007

mers. PEG exhibits several unique properties such as creating stealth conditions, which results in minimized interaction ability with the components of blood.[24] These characteristics enable PEG-coated particles to circulate in the blood for an extended period without being recognized by the body's defenses.[3] Therefore, the enhanced circulation time allows for preferential accumulation in affected areas of the body.[25,26]

The design of the gene delivery carrier is significant because the particle must be stable enough to resist extra and intracellular enzymes as well as allow penetration through the cell membrane. Several systems such as a block copolymers composed of DMAEMA and PEG, a random copolymer of DMAEMA and poly(ethyleneglycol) methacrylate (PEGMA), and DMAEMA-OligoEGMA have been studied previously.[12,27−29] These polymers showed a good ability to encapsulate genes. However, the micelles based on the above copolymers were reportedly not stable, with micelles disintegrating into unimers especially at high salt concentration.[27]

An easy and promising approach to target a more robust delivery system consists of cross-linking micelles to stabilize the aggregates against disintegration upon dilution or changes in the environment.[30−32] A range of pathways has been reported to achieve further stabilization of self-aggregates. The introduction of reactive or polymerizable end groups to the hydrophobic block of an amphiphilic block copolymer enables the fixation of the micelle within the micelle core.[33,34] Furthermore, the random distribution of functional groups along the hydrophobic block promotes the stabilization of the structure.[35] However, this approach limits the loading capacity and affects drug release. Shell-cross-linked micelles, so-called knedels, were first introduced by Wooley et al.[36,37] allowing the stabilization of the micelle without affecting the loading capacity in the core.[38,39]

Here, we employ the RAFT process[40−42] to stabilize self-assembled structures.[43,44,46] In this project, DMAEMA and PEGMA (M_n = 360 g mol^{-1}) were used to synthesize the block copolymer, PDMAEMA-*b*-P(PEGMA), using the RAFT process. Upon dissolution of these block copolymers in water, stimuli-responsive micelles were formed. The hydrophilic shell was further stabilized by cross-linking of the shell employing ethylene glycol dimethacrylate for chain extension via the RAFT process.[43,44]

Experimental Procedures

Materials. The RAFT agent 4-cyanopentanoic acid dithiobenzoate (4-CAD) was prepared according to the procedure described elsewhere.[45] Sodium hydroxide (Aldrich, 98%), HCl (Aldrich, 32%), Sodium chloride (Univar, reagent), and methanol (Univar, 99%) were used without any further purification.

2-(Dimethylamino) ethyl methacrylate (DMAEMA) (Aldrich, 98%), polyethyleneglycol methacrylate (M_n = 360 g mol^{-1}) (PEGMA) (Aldrich, reagent), and ethyleneglycol dimethacrylate (EGDMA) (Aldrich, *98%*) were destabilized by passing them over a column of basic alumina. 2,2-Azobisisobutyronitrile (Fluka, 98%) was purified by recrystallization from methanol.

The oligonucleotides (ISIS5132, sequence (5′-3′): TCCCGCCTGTGACATGCATT; molecular weight, 6363.9 g mol^{-1}) were purchased from Sigma. Ethidium bromide (Bio-Rad) was used as received.

Polymerization. *(a) Synthesis of Poly(2-(dimethylamino) ethyl methacrylate) (PDMAEMA).* 2-(Dimethylamino) ethyl methacrylate (35 g, 0.2226 mol), 4-cyanopentanoic acid dithiobenzoate (0.2473 g, 8.85 × 10^{-4} mol), and AIBN (0.0095 g, 8.85 × 10^{-5} mol) were combined with methanol (40 mL). The reaction mixture was divided equally into 10 vials. After sealing the reaction flasks, the mixture was purged with nitrogen for 1 h at 0 °C. The flasks were immersed in a water bath at 60 °C, and samples were taken over a period of 24 h. Polymerization was terminated by placing the sample bottles in an ice bath for 5 min. The polymer was purified by precipitation in cyclohexane and finally dried under reduced pressure.

(b) Synthesis of Poly(2-(dimethylamino) ethyl methacrylate-block-polyethylene glycol methacrylate) PDMAEMA-b-P(PEGMA). Two PDMAEMA samples with 120 and 150 repeating units were used as macro-RAFT agents for chain extension with PEGMA. The number of DMAEMA units was calculated from NMR results in combination with the theoretical number of repeating units as obtained from conversion. For PDMAEMA$_{120}$, 0.8936 g of PDMAEMA (M_{n120}(theo) = 19,000 g mol^{-1}; M_{n120}(SEC) = 9,200 g mol^{-1}, 4.7 × 10^{-5}mol (theo)), PEGMA (8.532 g, 0.0237 mol), and AIBN (0.00077 g, 4.7 × 10^{-6} mol) were dissolved in toluene to obtain a final volume of 20 mL. For PDMAEMA$_{150}$, 1.122 g of PDMAEMA$_{150}$ (M_{n150}(theo) = 23,833 g mol^{-1}; M_{n150}(SEC) = 12,500 g mol^{-1}, 4.7 × 10^{-5} mol), PEGMA (8.532 g, 0.0237 mol), AIBN (0.00077 g, 4.7 × 10^{-6} mol), and toluene were mixed. The solution was evenly separated in several Schlenk tubes, sealed with glass stoppers, and degassed with five freeze−pump−thaw cycles. Polymerizations were carried out at 60 °C in a water bath, and samples were taken out for different time intervals over a period of 2 h. Copolymers were purified using membrane dialysis for 2 days against distilled water and then freeze-dried.

(c) Micellization of PDMAEMA-b-P(PEGMA). The amphiphilic block copolymer PDMAEMA-*b*-P(PEGMA) was dissolved in distilled water at a concentration of 1 g L^{-1}. Equimolar amounts of HCl according to PDMAEMA units were added to PDMAEMA$_{120}$-*b*-P(PEGMA)$_{15/65}$ and PDMAEMA$_{150}$-*b*-P(PEGMA)$_{56/72}$ copolymer solution to obtain a fully protonated polymer. For other pH values, HCl or NaOH solutions were prepared to adjust the pH value.

(d) Chain Extension of Poly(2-(dimethylamino) ethyl methacrylate-block-polyethylene glycol methacrylate) (PDMAEMA-b-P(PEGMA)) with Ethylene Glycol Dimethacrylate (EGDMA) and Additional PEGMA. PDMAEMA$_{80}$-*b*-P(PEGMA)$_{100}$ (250 mg) (5.1 × 10^{-6} mol, M_n (theo) = 49,000 g mol^{-1}) and 15 mg of PEGMA (4.16 × 10^{-5} mol) were added to 200 mL of distilled water. The mixture was stirred at 0 °C for 1 day and covered with aluminum foil (to avoid UV initiated polymerization). EGDMA (1.035 mg) (5.15 × 10^{-6} mol) and 0.375 mg of 4,4′-azo-bis(4-cyano-pentanoic acid) (ACPA) (1.33 × 10^{-6} mol) were dissolved in 50 mL of acetone and then transferred to a 500 mL Schlenk flask with the solution described above. The mixture was degassed via five consecutive freeze−pump−thaw cycles, stirred at 0 °C for 2 h, and then immersed in a water bath at 60 °C for 48 h. Finally, the product was purified using membrane dialysis for 2 days against distilled water and then dried under vacuum using a freeze dryer.

Analysis. *Nuclear Magnetic Resonance (NMR) Spectroscopy.* All NMR spectra were recorded using a Bruker 300 MHz spectrometer. The RAFT agent (4-CAD) and PDMAEMA were analyzed using $CDCl_3$, and the block copolymer and the cross-linked micelles were analyzed in *d*-DMSO or D_2O.

Size Exclusion Chromatography (SEC). Molecular weight distributions of the block copolymers were determined by size-exclusion chromatography (SEC) using a Shimadzu modular system, comprising an auto-injector, a Polymer Laboratories 5.0 μm bead-size guard column (50 × 7.5 mm), three linear PL columns (10^5, 10^4, and 10^3 Å), and a differential refractive index detector. The eluent was *N*,*N*-dimethylacetamide (DMAc) (0.03% w/v LiBr, 0.05% w/v BHT) at 40 °C with a flow rate of 1 mL min^{-1}. The system was calibrated using narrow polystyrene standards ranging from 500 to 10^6 g mol^{-1}.

The RAFT agent 4-CAD and PDMAEMA were analyzed on a similar SEC system at 25 °C using THF as the mobile phase. Narrow polystyrene standards ranging from 500 to 10^6 g mol^{-1} were employed.

Surface Tensiometer. The critical micelle concentration (CMC) was determined by analyzing the surface tension using a NIMA DST 9005 Dynamic Surface Tensiometer with a Pt/Ir Nouy ring at 25 °C.

Dynamic Light Scattering (DLS). Particle sizes were determined using a Brookhaven Zetaplus particle size analyzer (laser, 35 mW; λ

= 632 nm; angle, 90°) and a solution of polymer above CMC in water at 25 °C. Samples were purified from dust using a microfilter (0.45 μm) before analyzing. The mean diameter was obtained from the arithmetic mean using the relative intensity of each particle size.

Transmission Electron Microscopy (TEM). The TEM micrographs were obtained using a Hitachi H7000 transmission electron microscope. The samples were prepared by casting the solution onto a copper grid. No additional staining was employed.

Ethidium Bromide Displacement Assay. The ethidium bromide displacement assay was prepared according to the methods described earlier.[5] Excitation wavelength (λ_{ex} = 480 nm) and emission wavelength (λ_{em} = 605 nm) of ethidium bromide (EtBr) were obtained using a Perkin-Elmer LS50B scanning instrument employing a slit width at 5 nm at five different concentrations. The fluorescence of EtBr (2 μg mL^{-1}) was initially measured, and 10 μg of ON was then added. An aliquot of block copolymer and cross-linked micelles was then titrated into the solution corresponding to various polymer/ON molar ratios. The relative fluorescence was calculated as follows:

$$\%\ \text{relative fluorescence} = \frac{fluorescence(Obs) - fluorescence(EtBr)}{fluorescence(ON + EtBr) - fluorescence(EtBr)}$$

Cell Assays. The cytotoxicity of (a) cumyl dithiobenzoate (CDB), (b) polystyrene prepared using CDB, (c) PDMAEMA prepared using 4-CAD, and (d) the cross-linked micelle was quantified using cell line L929 (see Supporting Information for details).

Results and Discussion

(a) PDMAEMA-*b*-P(PEGMA) Block Copolymers: Synthesis and Characterization. *Synthesis of PDMAEMA-b-P(PEGMA) Block Copolymers.* RAFT polymerization was shown to be a suitable method to prepare cross-linked micelles by utilizing the thiocarbonylthio group attached to each polymer chain to carry out a chain-extension experiment using a cross-linker. This technique has been widely employed to cross-link the core[43,46] or the nexus between both blocks,[44] whereas here, we attempt to stabilize the shell via cross-linking. It is therefore essential to have the thiocarbonylthio group located at the surface of the micelle. Consequently, because of the mechanism of RAFT polymerization, the first block is required to be the hydrophobic block. The targeted micelles have specific structures with DMAEMA block as the core and PEGMA block as the shell, and therefore, the DMAEMA block was synthesized first, and the resulting macromolecular RAFT agent was further chain-extended with PEGMA. After self-assembly in an aqueous environment, the shell was cross-linked with the addition of ethyleneglycol dimethacrylate facilitated by further addition of PEGMA.

PDMAEMA macroRAFT agents were generated using methanol as the solvent. The choice of the solvent has been previously shown to have a significant influence on transesterification effects of the monomer.[47] However, no detectable amount of methyl methacrylate units has been obtained during the RAFT polymerization as confirmed using ^{1}H NMR. The polymerization was found to proceed according to first-order kinetics, indicating a constant radical concentration while inhibition periods were absent. SEC profiles (Figure 1) display the evolution trace of PDMAEMA with conversion. The SEC chromatograms suggest the absence of noticeable side reactions, while the molecular weight distribution remains narrow (PDI < 1.2) throughout the course of the polymerization. A high molecular weight shoulder appears at high conversions, which may be assigned to unknown side reactions. Termination by combination is usually of minor

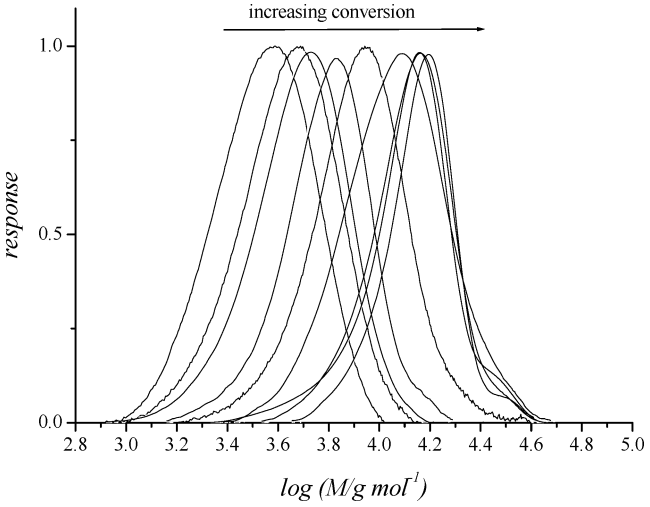

Figure 1. Molecular weight distribution as obtained from SEC of the polymerization of DMAEMA in methanol at 60 °C ([DMAEMA] = 3 mol L^{-1}, [4-CAD] = 1.2 × 10^{-2} mol L^{-1}, [AIBN] = 7.7 × 10^{-4} mol L^{-1}); the monomer conversions are 25.9%, 27.6%, 31.1%, 32.4%, 46.2%, 53.8%, 59.6%, 60%, and 64.5% (reaction times 1 to 24 h).

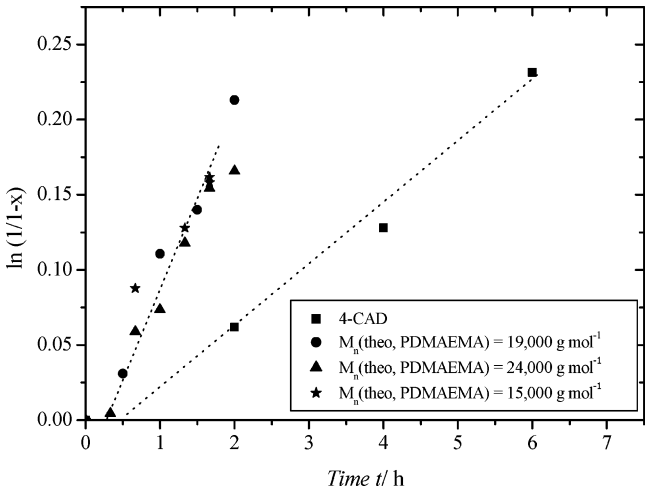

Figure 2. First-order kinetic plot of the polymerization of poly(ethylene glycol) methacrylate PEGMA at 60 °C in the presence of 4-CAD and varying PDMAEMA macroRAFT agents ([PEGMA] = 1.33 mol L^{-1}, [RAFT groups] = 2.65 × 10^{-3} mol L^{-1}, [AIBN] = 2.65 × 10^{-4} mol L^{-1} in toluene).

importance in methacrylate polymerizations and cannot be the cause of high molecular weight products.

The chain extension to form block copolymers has to be exercised with caution. Loss of RAFT endgroups by UV-light, peroxides, hydrolysis, or heat has to be avoided.[50] In addition, it has to be considered that radicals generated by AIBN can result in the formation of homopolymers during block copolymer synthesis. The initial AIBN concentration was therefore kept well below the RAFT agent concentration. Taking the slow decomposition of AIBN at 60 °C into account, the amount of homopolymer can therefore almost be neclegted.

Prior to the chain extension of the PDMAEMA macroRAFT agent with PEGMA, the RAFT (homo)polymerization of PEGMA was investigated using 4-cyanopentanoic acid dithiobenzoate (4-CAD). The polymerization kinetics are best represented by a first-order kinetic plot (Figure 2) while the molecular weights increased linearly with conversion. However, the polymerization could only be carried out to a conversion of around 20% accompanied by the formation of gel particles. This cross-linking process is probably caused by transesterification

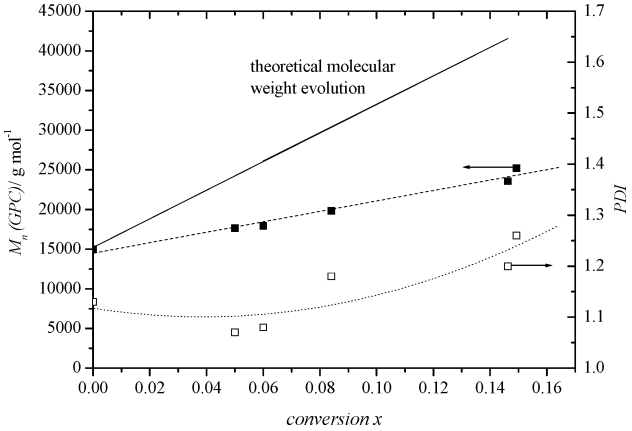

Figure 3. Number-average molecular weight M_n as obtained with SEC and polydispersity index (PDI) vs monomer conversion x of the polymerization of poly(ethylene glycol) methacrylate at 60 °C in the presence of PDMAEMA macroRAFT agent (M_n = 15,000 g mol^{-1}) ([PEGMA] = 1.33 mol L^{-1}, [RAFT groups] = 2.65 × 10^{-3} mol L^{-1}, [AIBN] = 2.65 × 10^{-4} mol L^{-1} in toluene).

processes, which are typical for these types of monomers. In addition, the commercially available monomer is known to contain trace impurities of poly(ethylene glycol) dimethacrylate, which can undergo cross-linking.[48] The molecular weights measured were considerably smaller than the theoretical molecular weights as a result of the polystyrene SEC calibration and noticeably smaller hydrodynamic volumes of branched polymers. However, high molecular weight byproducts were clearly absent, and the very narrow molecular weight distribution with polydispersity indices PDI of 1.15 may suggest a controlled/living system. A range of PDMAEMA macroRAFT agents with different molecular weights (15,000 to 24,000 g mol^{-1}) was further employed for chain extension using PEGMA. The polymerization was found to proceed noticeably faster in the presence of a PDMAEMA chains (Figure 2). This phenomenon has been previously reported showing that the size of the macroRAFT agent can have a significant influence on the rate of polymerization.[44,49] To date, the origin of this effect is unknown; however, a reduction of termination events due to increased viscosity of the large macroRAFT agent can be given as one possible explanation.[50]

SEC curves as well as the linear correlation between molecular weight and PEGMA conversion seem to confirm the livingness of the system (Figures 3 and 4). Upon closer inspection of the SEC curves, a slight broadening of the curve can be observed, which is reflected by the increase in polydispersity to 1.3 at higher conversions. The presence of a slight molecular weight tailing probably reveals some incomplete PEGMA chain extension. To further investigate this observation, the intensity of the GPC curves were recalculated to take into consideration that with increasing PEGMA conversions the intensity of the original PDMAEMA macroRAFT block was skewed.[49] The intensity of each GPC curve was multiplied with the theoretical number of repeating units of the block copolymer $N_{DMAEMA} + N_{PPEGMA}$ and divided by the size of the original macroRAFT agent $N_{PDMAEMA}$. (It should be noted that this technique can only provide an estimate, given that both polymer blocks deviate in their refractive indices.) It seems that a slightly delayed consumption of the PDMAEMA macroRAFT agent is observed indicative of a hybrid behavior. This observation is quite typical for many complex architectures and is discussed in detail elsewhere.[49,50]

However, the molecular weight increased linearly with conversion. The significant deviation of the theoretical molecular

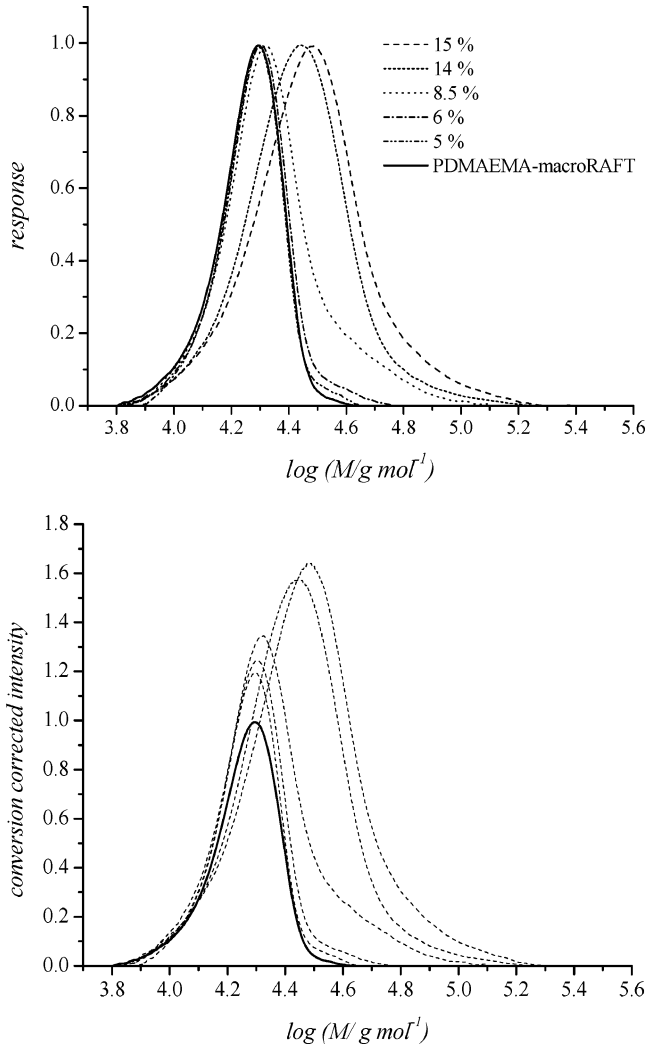

Figure 4. Molecular weight distribution as obtained from SEC of the polymerization of poly(ethylene glycol) methacrylate at 60 °C in the presence of PDMAEMA macroRAFT agent (M_n (theo) = 15,000 g mol^{-1}) ([PEGMA] = 1.33 mol L^{-1}, [RAFT groups] = 2.65 × 10^{-3} mol L^{-1}, [AIBN] = 2.65 × 10^{-4} mol L^{-1} in toluene). Above, normalized distribution; below, intensity of distribution corrected by conversion of PEGMA.

weight from the value obtained via SEC can be considered to be a result of the linear polystyrene calibration employed to determine the molecular weight of the synthesized block copolymers.

Self-Assembly of PDMAEMA-b-PEGMA. While PDMAEMA can dissolve readily in water, it still shows some strong hydrophobic tendencies, especially at high pH values when the polymer is not protonated. Water as a selective solvent therefore forces PDMAEMA-*b*-P(PEGMA) to self-assemble with P(PEGMA) forming the water-soluble shell. The size and shape of the aggregates are typically dependent on block lengths and ratio, resulting in the formation of aggregates such as vesicles, micelles, or rods.[51−53] Four block copolymers $PDMAEMA_{120}$-$P(PEGMA)_{15/65}$ and $PDMAEMA_{150}$-$P(PEGMA)_{56/72}$ were chosen to study the effects of block length on aggregation behavior and the stability of the self-assembled system.

pH Responsibility. Driven by the reversible protonation of the DMAEMA block, the size of the self-assembled aggregate changes according to the pH value of the surrounding environment. This stimuli-responsive alteration of the particle size of the aggregate dependent on the pH value can be observed using dynamic light scattering (DLS) (Figure 5).

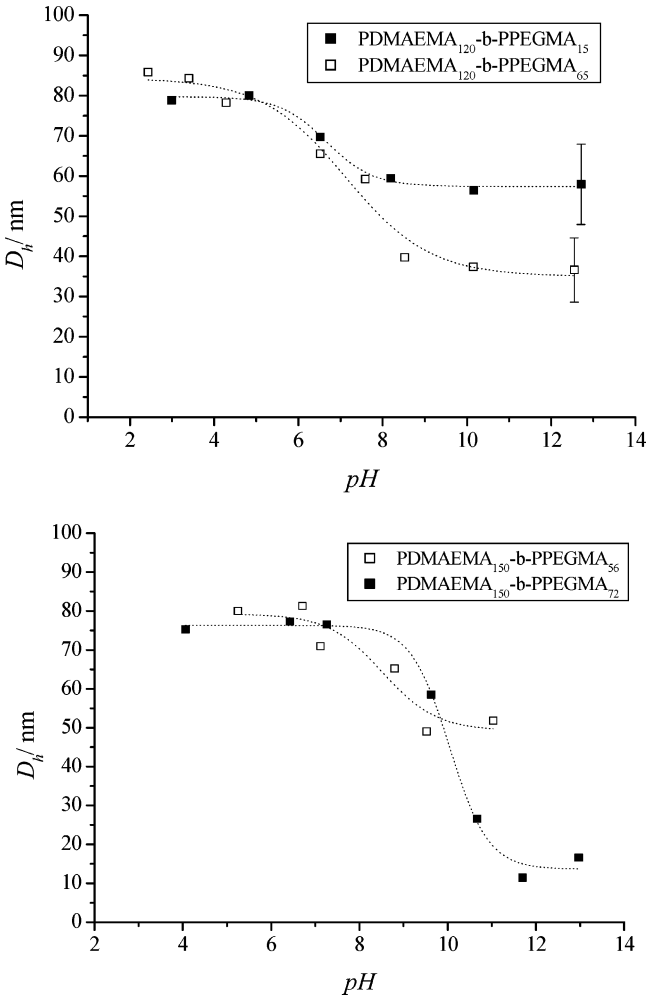

Figure 5. Hydrodynamic diameter D_h as obtained using DLS vs pH value of PDMAMEA-*b*-P(PEGMA) block copolymers in aqueous solution at 25 °C on the basis of $PDMAEMA_{120}$ (above) and $PDMAEMA_{150}$ (below) macroRAFT agents.

Low pH. DMAEMA has weak basic amine end groups, which are protonated at low pH; thus, a high degree of ionization occurs. In contrast to earlier reports suggesting the dissolution into unimers upon protonation,[27−29] the self-assembly here was found to be stable at low pH values. This unexpected stability was suspected to be the result of having carboxy end groups of the RAFT agents located within the core, which can potentially form strong interactions with the DMAEMA amino group. More details will be introduced later. The size below 100 nm indicates the formation of micelles. Interestingly, the size of these micelles (around 80−90 nm) appeared to be independent of the P(PEGMA) block length. Ionized DMAEMA blocks exhibit charge−charge repulsion within each micelle leading to their expansion.

Neutral Region. As the pH increases, the concentration of $[H^+]$ drops subsequently, resulting in the deprotonation of the amine groups. Consequently, the repulsive forces decline and lead to the contraction of the micelles as observed by the decrease of the micelle size. While the pK_a of DMAEMA is reportedly 7.3,[54] the point of inflection can vary depending on the architecture of the polymer.[55] A variation of the pK_a value of the self-assembled aggregate can indeed be observed in the studied system. With increasing PDMAEMA block size, the pK_a value is pushed to higher values (>8.4). With the protonation of PDMAEMA, the charge density along the polymer increases, preventing further acid−base reaction. However, the correlation between pH value and particle size can only give an indication about the protonation of DMAEMA but cannot be set equivalent to pK_a determination via acid−base titration.

High pH. With increasing pH, the amino groups are gradually deprotonated until complete deionization of the PDMAEMA blocks. A collapsed conformation is observed in the absence of charge−charge repulsion. The hydrophobic features of the PDMAEMA block result in even more compact structures, until maximum attraction among the hydrophobic blocks is achieved. It seems that the longer the P(PEGMA) block, the bigger the differences in hydrodynamic size when comparing low and high pH values.

The relationship between hydrophobic and hydrophilic block sizes does not correlate with the obtained hydrodynamic diameter as predicted by scaling theories as established by Noolandi and Hong[56] or Halperin.[57] In contrast to these mathematical models, the hydrodynamic diameter does not increase with increasing hydrophobic block length. This behavior can probably be assigned to the strong hydrophilic character of the core-forming DMAEMA, which results in a weakly segregated block copolymer system.

This interpretation of contraction and expansion is basing on the assumption that the number of polymer chains per micelle is constant. However, as the micelles are in equilibrium with each other, the change in the size can also be due to a change of number of polymer chains per micelle.

Critical Micelle Concentration (CMC). CMC was determined via surface tension analysis. At low concentration, the amphiphilic block copolymers readily spread on the surface, affecting the surface activity at the air/water interface; therefore, the surface tension of the polymer solution decreases immediately. Once the maximum capacity of the surface has been reached, micelle formation is observed as expressed via the CMC (critical micelle concentration). The CMC of a range of amphiphilic block copolymers were determined in water at 25 °C (Figure 6).

The CMC of $PDMAEMA_{120}$-*b*-$P(PEGMA)_{15}$, $PDMAEMA_{120}$-*b*-$P(PEGMA)_{65}$, $PDMAEMA_{150}$-*b*-$P(PEGMA)_{56}$, and $PDMAEMA_{150}$-*b*-$P(PEGMA)_{72}$ were 0.00045 mg mL^{-1} (1.8×10^{-5} mol mL^{-1}), 0.0024 mg mL^{-1}(5.7×10^{-5} mol mL^{-1}), 0.0011 mg mL^{-1}(2.5×10^{-5} mol mL^{-1}), and 0.0031 mg mL^{-1}(6.2×10^{-5} mol mL^{-1}), respectively. It is evident that with increasing hydrophilic block length, the polymers show a smaller tendency to aggregate. The effect of the length of the hydrophobic DMAEMA block is too insignificant here to be discussed, but there is a slight indication that the CMC declines with increasing length of PDMAEMA.

As shown in Figure 6, fluctuation of surface tension appeared even when the concentration was beyond CMC. Instabilities in the measurements may be assigned to the fact that the time interval (30 min) is not sufficient for the system to reach equilibrium. The time required to reach equilibrium in a block copolymer system can be substantial[58] with equilibrium times of 10 h up to years being reported.[59] However, we exclude this possibility since the changing trend was similar in all studies, and repeated measurements revealed the reproducibility of these results independent of the equilibrium time. A possible explanation for the sudden increase of the surface tension after the CMC has been reached stems from the nature of the basic DMAEMA block. DMAEMA is a weak polyelectrolyte, and the tertiary amino groups are partly protonated in an aqueous environment.[60] With a further addition of polymer, increasingly repulsive charges in the PDMAEMA block push the polymer away from the air/water surface, leading to an increase in surface tension. At higher polymer concentrations, the change in charge density

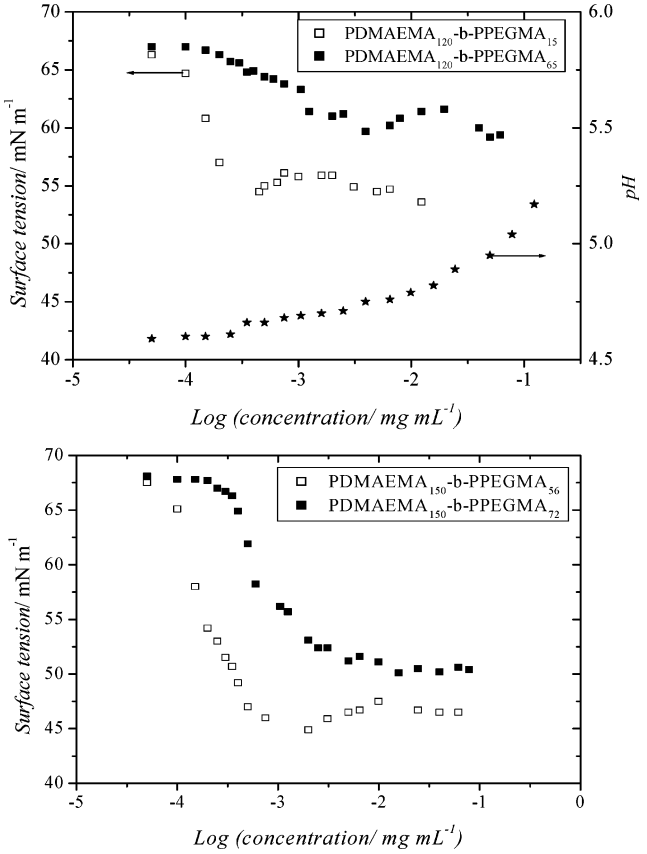

Figure 6. Surface tension vs concentration of PDMAMEA-*b*-P(PEGMA) block copolymers in aqueous solution at 25 °C on the basis of $PDMAEMA_{120}$ (above) and $PDMAEMA_{150}$ (below) macroRAFT agents. The upper graph includes the evolution of the pH value with added block copolymer $PDMAMEA_{120}$-*b*-$P(PEGMA)_{40}$ (★).

becomes negligible. Additional polyelectrolyte cannot enter the micelles; thus, they assemble together and form new free micelles. Therefore, the surface tension decreases slightly. This is a dynamic equilibrium, an interaction between intramolecular and intermolecular associations.[58] On this note, the pH value with increasing block copolymer was recorded, resulting in vital information regarding the protonation of the block copolymer. The deionized water used, obtained using ionic exchange resins, typically shows a pH value below 7 and is therefore slightly acidic. Added PDMEAMA does not significantly change the pH value (Figure 6), keeping the pH value therefore well below the pK_a value of PDMAEMA. The polymer is therefore highly protonated during the course of the experiment; Figure 6 consequently displays the behavior of the block copolymer in its charged state. Alternatively, measurements can be carried out using buffer solutions. It should, however, be considered that high ionic strength will noticeably interfere with the aggregation of block copolymers.

It should also be noted that the length of both blocks have a noticeable influence on surface tension. Longer P(PEGMA) blocks will increase the surface tension, while longer hydrophobic PDMAEMA blocks will result in a significant decrease (Figure 6). Therefore, block copolymers with a considerable content of hydrophobic sequences exhibit a higher surface activity.

TEM Analysis. TEM studies were employed to confirm DLS results and to obtain information on the shape of these aggregates. Figure 7 reveals the typical core−shell structure of a micelle with the PDMAEMA blocks appearing dark even without additional staining of the sample. As summarized in Table 1, significant differences in particle size were observed at high and low pH values. The micelle sizes range between 75 and 90 nm in the protonated state, while the particles size drops to values around 14 to 56 nm at high pH values and are therefore in an order of magnitude similar to that of the DLS measurements (Note: a generous error of 20% was given for the analysis of the diameter of core and shell.) It should, however, be considered that TEM presents the particle size in the solid state and not the hydrodynamic diameter as obtained via DLS. The core of the micelles could clearly be distinguished from the corona by its darker appearance. The size of the core could therefore be estimated with values of around 50 nm at low pH and 25 nm at high pH values. Investigation of the core size reveals that the core has indeed a significantly higher diameter in its protonated state (Table 1). As suspected earlier, the increase in particle size at low pH values can be derived by repulsive forces within the core on the basis of the high charge density.

Investigation via NMR. So far, it seemed very unusual to observe the formation of stable micelles at low pH values. While DLS and TEM studies seemed to indicate that these aggregates were indeed present, further analysis is required. Additional information on the chain mobility and thus the micellar structure was provided by NMR studies. The limited mobility of the core-forming blocks in aqueous solution results in the broadening or the complete disappearance of the corresponding peaks.[61] Earlier NMR studies on a PDMAEMA based polymer using varying temperatures and pH values could confirm the formation of unimers and micelles, respectively, upon external stimuli.[62−64] Significant signal shifts of the methyl and methylene groups directly attached to the nitrogen were observed after protonation. In addition, the intensity of this signal declined, accompanied by broadening when the DMAEMA block took on the role of the hydrophobic core of the micelle. Therefore, a block copolymer, $PDMAEMA_{80}$-*b*-$P(PEGMA)_{100}$, with a theoretical ratio between the integrals of the PDMAEMA peak (− N(CH_3)$_3$), $\delta \approx 2.32-2{,}92$ ppm) and the PEGMA peak (O-(CH_2)$_2$-O, $\delta \approx 3.63$ ppm) of 0.43, was investigated at 25 °C. By adjustment of the pH value with hydrochloric acid to 4, the PDMAEMA peak became very sharp and shifted from $\delta \approx 2.32$ ppm to $\delta \approx 2.92$ ppm because of the protonation of tertiary amino groups in PDMAEMA in the acidic environment. The experimental ratio was found to be equal to 0.15 (a significant ratio reduction from 0.43), indicating the reduced movement of the PDMAEMA block within the core. As the pH value increased to pH 7, the protonation effect disappeared, and the peak assigned to the six dimethylamino protons of PDMAEMA reappeared at $\delta \approx 2.32$ ppm. Further increase of the pH value to 12 does not provoke a further shift, but an additional decrease of the ratio of the intensity of the area integrals of the DMAEMA signals from 0.10 (pH 7) to 0.07 (pH 12) is observed. The deprotonation of the PDMAEMA block leads therefore to an increased hydrophobicity, thus to a decrease in chain dynamics.[65] The signal at low pH value appears to be sharp, which is rather unusual for the core-forming block. This is usually an indication of the hydration of these amino groups resulting in micelles with a water swollen core.

(b) Why Are These Micelles So Stable at Different pH Values? In contrast to the stimuli-responsive block copolymers used in many reports, these block copolymers do not show any indication of forming unimers at $C >$ CMC, when protonated. Independent from the pH value, the micelles do only vary in diameter size, but unimers are fully absent. Typically, block copolymers consisting of a fully water-soluble block and a pH-

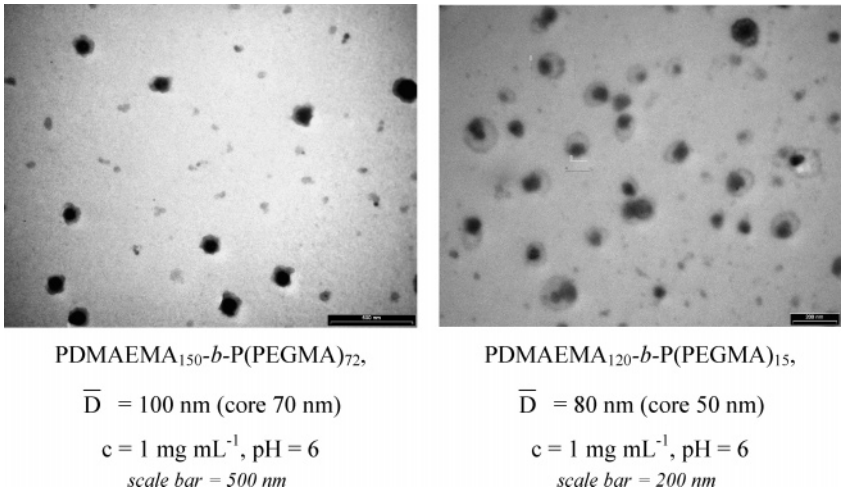

Figure 7. TEM pictures obtained from two different block copolymers.

Table 1. Particle Sizes Measured by TEM of $PDMAEMA_{120}$-*b*-$P(PEGMA)_{15}$, $PDMAEMA_{120}$-*b*-$P(PEGMA)_{65}$, $PDMAEMA_{150}$-*b*-$P(PEGMA)_{56}$, and $PDMAEMA_{150}$-*b*-$P(PEGMA)_{72}$ Cast from Aqueous Medium (1 mg mL^{-1}) at Different pH Conditions

	particle diameter D/core diameter (nm) ± 20%	
block copolymer	at low pH (<pH 5)	at high pH (>pH 10)
$PDMAEMA_{150}$-*b*-$P(PEGMA)_{72}$	80/50	50/25
$PDMAEMA_{150}$-*b*-$P(PEGMA)_{56}$	85/50	55/30
$PDMAEMA_{120}$-*b*-$P(PEGMA)_{65}$	85/50	40/25
$PDMAEMA_{120}$-*b*-$P(PEGMA)_{15}$	90/65	50/25

responsive block display the full disintegration into unimers in their protonated state while forming aggregates in their neutral state. The unusual behavior in this case can potentially only be explained by the presence of carboxy end groups, which are introduced by the RAFT agent as a part of the leaving group. These acid groups are located within the core and can therefore undergo strong interaction with the DMAEMA amino group. To test this hypothesis, an additional block copolymer was synthesized using a nonpolar RAFT agent, cumyl dithiobenzoate CDB. Since the RAFT agents are of similar structure with equivalent stabilities of the Z- and R-groups, the observed kinetic behavior in the synthesis of these block copolymers is comparable. The resulting block copolymer was now processed in a similar manner. As a consequence of the disappearance of the carboxy group, the hydrodynamic diameter now indicated the formation of unimers at low pH value. While this block copolymer, $PDMAEMA_{80}$-*b*-$P(PEGMA)_{55}$ prepared using CDB, displayed a hydrodynamic diameter (DLS) of 67 nm at pH 12, only a single signal corresponding to a size of 7 nm appeared at pH 2. It seems, therefore, that strong H bonds have led to a micellar system that can withstand pH changes. To break down these interactions, a block copolymer, $PDMAEMA_{120}$-*b*-$P(PEGMA)_{40}$ prepared using 4-CAD, was dissolved in an aqueous solution containing varying amounts of urea. Urea is known to ease the strength of these H bonds, allowing a better dissolution. Indeed, with increasing amounts of urea, the particle size declines, leveling off at a urea concentration of 6 mol L^{-1} (Figure 9) confirming the strong interaction caused by the functional RAFT agent used.

It seems therefore that the presence of the carboxy group results in the formation of strong interaction leading to stable micelles. To further test this hypothesis, a PDMAEMA homopolymer with 120 repeating units was investigated at varying pH values. In the unprotonated state at pH 12, $PDMAEMA_{120}$, prepared using 4-CAD as RAFT agent, has a particle size of 46 nm, which is significantly larger than that expected for a single polymer chain. Even at very low pH values (pH < 2),

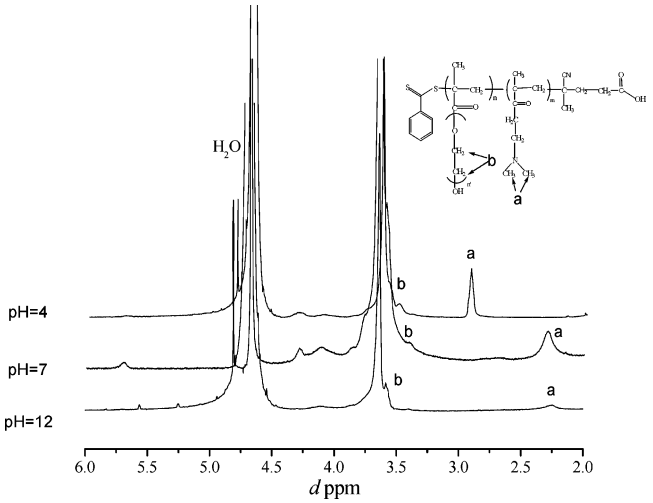

Figure 8. ^1H NMR spectra for $PDMAEMA_{80}$-*b*-$P(PEGMA)_{100}$ block copolymer at 25 °C in D_2O at pH 4, 7, and 12.

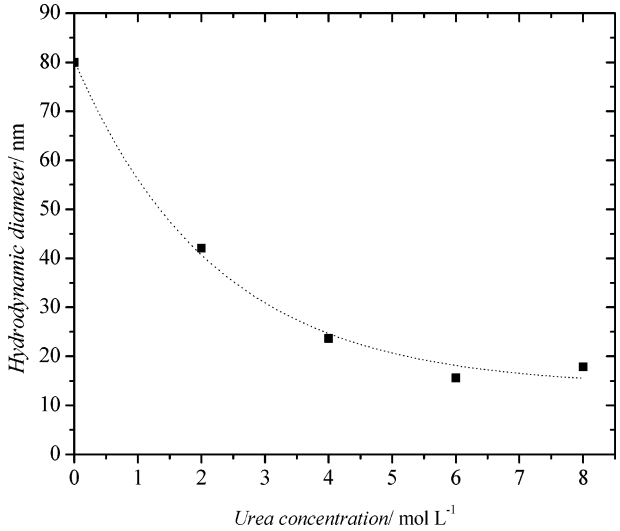

Figure 9. Hydrodynamic diameter as obtained via DLS of an aqueous solution of $PDMAEMA_{120}$-*b*-$P(PEGMA)_{40}$ (1 mg mL^{-1}, pH 2) dependent on added urea.

Scheme 1. Synthetic Approach to the Synthesis of Shell-Cross-linked Micelles

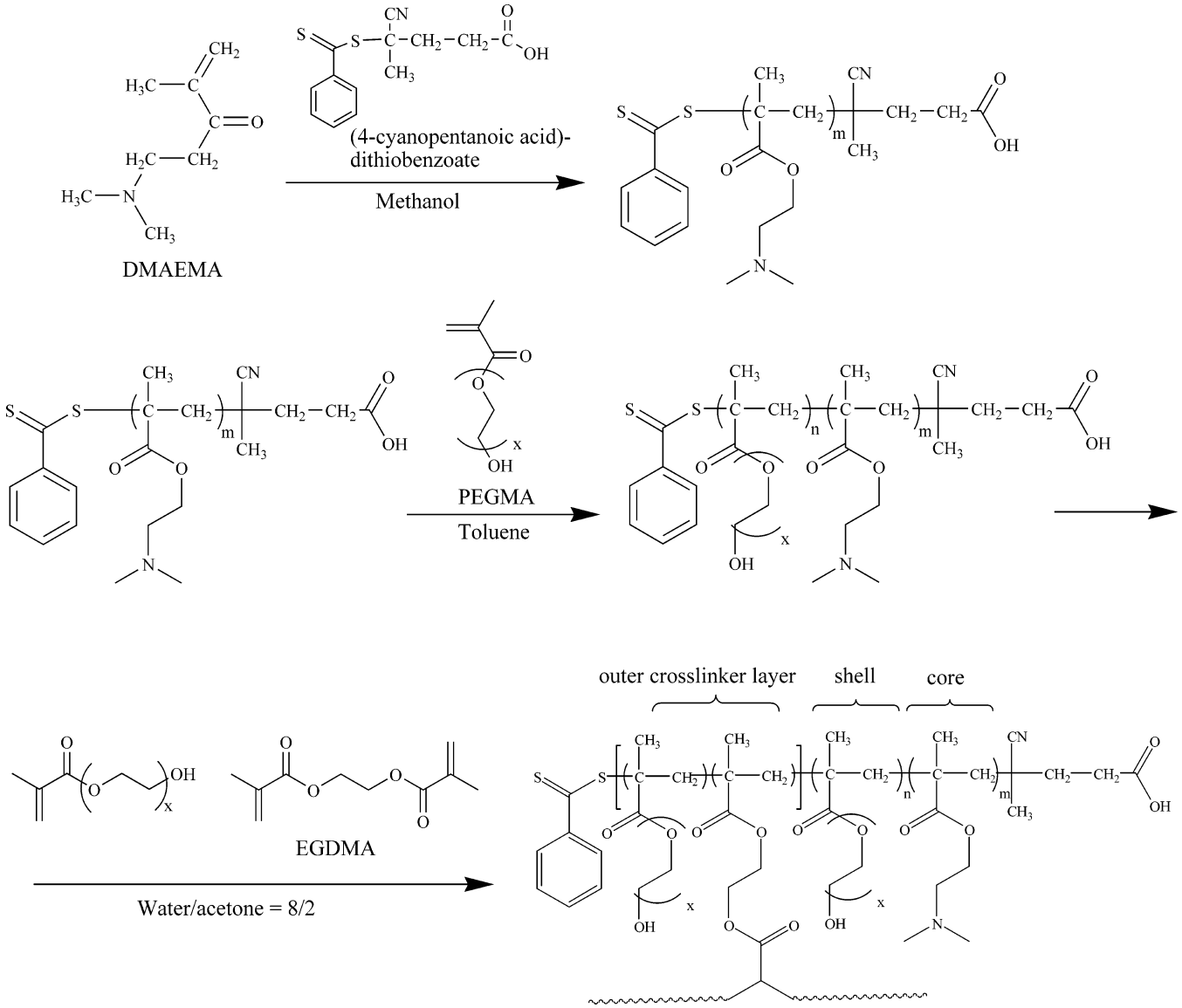

when all the DMAEMA repeating units are expected to be in their cationic form, the hydrodynamic diameter was observed to be around 52 nm. Both values have been confirmed by TEM studies. PDMAEMA with carboxy end groups is therefore never found in its unimeric state in contrast to PDMAEMA without any interactive end groups.

(c) Shell-Cross-Linked Micelles via RAFT Polymerization: Synthesis and Characterization. *Polymerization.* Further stabilization of the self-assembled core−shell structure can be achieved via chain extension of the block copolymer employing a divinyl compound as a cross-linking agent as proposed in Scheme 1.[43,44,66] In contrast to earlier studies where cross-linking was obtained within the micelle, the shell cross-linking is subject to severe limitations such as the possible covalent cross-linking between two or more micelles. To prevent such side reactions, cross-linking was carried out in highly diluted solutions. Furthermore, the cross-linker, ethylene glycol methacrylate (EGDMA), was diluted by the addition of a PEGMA monomer. The conditions were then optimized by variations of the ratio of EGDMA and PEGMA. The cross-linked products were investigated using SEC analysis. A known concentration of the cross-linked polymer was filtered with a 0.45 μm filter to remove any possible gel-like particles, which could have been formed during intermicellar cross-linking. The molecular weight (using a system calibrated with polystyrene standards) and the amount of cross-linked polymer (using the area integral of the filtered polymer, which indicates the amount of gel from intermicellar cross-linking) were utilized to draw conclusions concerning the cross-linking process.

The cross-linking process was attempted in pure water. However, the limited solubility of EGDMA in water resulted in a small fraction of cross-linked micelles next to a dominant amount of uncross-linked block copolymer. This behavior could not be improved by altering the PEGMA/EGDMA ratio. Organic solvents were therefore added to the reaction mixture to ensure good solubility of all components. However, it is essential to confirm that the formation of the self-assembled structure is not disturbed by the presence of cosolvents. A solvent composition with an added 20 vol % of acetone was then employed to achieve good solubility of all of the components while maintaining the micellar structure (confirmed using DLS at 60 °C). The chosen reaction conditions afforded the shell cross-linking of the micelles while preventing the formation of intermicellar structures. In addition, a molar ratio of EGDMA to PEGMA of 1:8 was sufficient to ensure an efficient cross-linking of the

Table 2. Molecular Weight Analysis via SEC (vs PS Standards) and Hydrodynamic Diameter Analysis via DLS (1 mg mL^{-1}) of the Shell-Cross-Linking of $PDMAEMA_{80}$-*b*-$P(PEGMA)_{100}$ via Chain Extension vs Reaction Time[a]

			SEC results			
	reaction time (h)	conversion (NMR)	M_n (g mol^{-1})[b]	PDI	peak area[c]	D_h in DMAc (nm)
block copolymer	–	–	50000	1.24	100%	7.1
cross-linked micelles (1)	17	62%	106000	1.44	23%	74
cross-linked micelles (2)	24	69%	81000	1.68	43%	67
cross-linked micelles (3)	48	82%	77000	1.99	84%	57

[a] $[PDMAEMA_{80}$-*b*-$P(PEGMA)_{100}] = 2 \times 10^{-5}$ mol L^{-1}, $[PEGMA] = 1.7 \times 10^{-4}$ mol L^{-1}, $[EGDMA] = 2 \times 10^{-5}$ mol L^{-1}, $[ACPA] = 5.3 \times 10^{-6}$ mol L^{-1} in Water/Acetone (4/1 v/v) at 60 °C. [b] Block copolymer: M_n (NMR) = 48,500 g mol^{-1}; $PDMAEMA_{80}$-*b*-$P(PEGMA)_{100}$. [c] A solution with a polymer concentration of 5 mg mL^{-1} was prepared followed by filtration using a filter with a pore size of 0.45 μm, which eliminates higher aggregates, resulting in smaller peak intensity. The area of the SEC signal was then compared to the block copolymer, which allows us to form conclusions regarding the formation of insoluble particles.

micelles, while higher concentrations of cross-linker (or less PEGMA) led to cross-linked gel-like particles.

The cross-linking process was followed in more detail using NMR, SEC, and DLS studies. Block copolymer, together with PEGMA and ethylene glycol dimethacrylate (EGDMA), was dissolved in deionized water and acetone. Prior to polymerization, the mixture was stirred at 0 °C to allow equilibration of the system. The polymerization proceeded at 60 °C for a preset time, followed by evaporation of the solvent and the determination of the monomer conversion via NMR (using tetramethylsilane as the internal standard). After a reaction time of 1 day, around 70% of double bonds were consumed (Table 2). Further polymerization up to 3 days did not significantly increase the overall conversion of PEGMA and EGDMA. However, inspection of the evolution of the molecular weights via SEC and the hydrodynamic diameter D_h via DLS in DMAc (a good solvent for both blocks) with reaction time reveals an interesting effect during an extended reaction period. A cross-linking time of 17 h resulted in an immediate molecular weight increase. It should be noted here that the molecular weights are calibrated using polystyrene standards and can therefore only be used as a measure for the alteration of the hydrodynamic volume. The peak intensity was rather weak (compared to a solution of block copolymer with exactly the same concentration) indicative for the removal of particles with diameters higher than 0.45 μm (pore size of filter) during the filtration process. At the same time, the particles size obtained via DLS indicated the formation of stable particles, while unimers are fully absent. Since DMAc is a good solvent for both blocks, this behavior can clearly be assigned to the stabilization of the micelle via cross-linking. Further cross-linking up to 3 days, however, does result in the reduction of the measured molecular weight, indicative of a smaller hydrodynamic volume. The alteration of the hydrodynamic volume was additionally confirmed using light-scattering studies with the hydrodynamic diameter declining with increasing reaction time. It seems, therefore, that an increase in cross-linking time leads to more compact structures.

It is interesting to note that the intensity of the SEC signal increases dramatically with increasing conversion. More particles are therefore present in the solution, which were not removed by filtration. This trend probably stems from a higher stability of the cross-linked micelles against intermicellar aggregation with proceeding reaction. The presence of aggregates (around 500 nm) was indeed confirmed by DLS. These aggregates could easily be eliminated by treatment with ultrasound for brief periods, but they tend to form again within a short time.

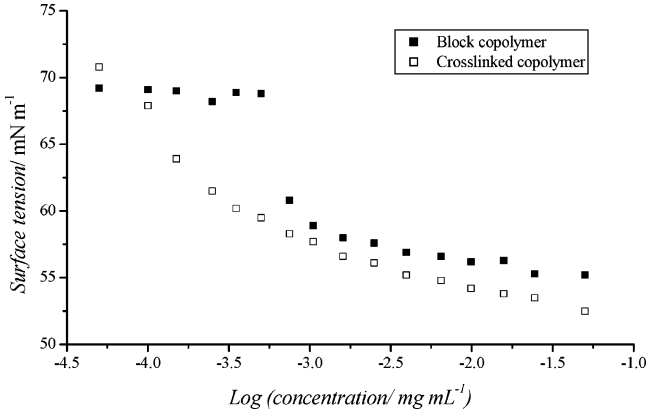

Figure 10. Surface tension vs concentration of $PDMAEMA_{80}$-*b*-$P(PEGMA)_{100}$ and its cross-linked counterpart in aqueous medium at 25 °C; pH 4.5−5.

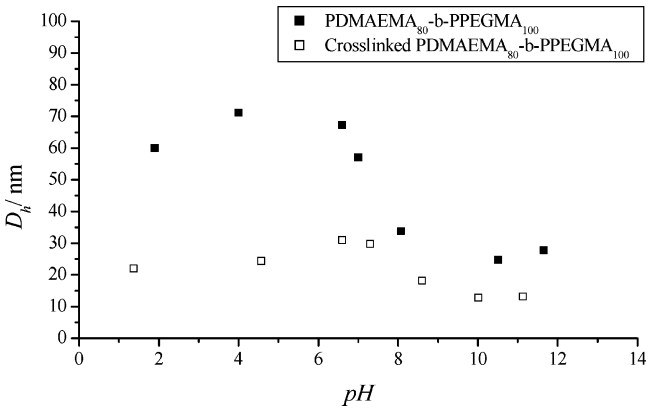

Figure 11. Comparison of hydrodynamic diameter D_h vs pH value in aqueous medium of uncross-linked and cross-linked $PDMAEMA_{80}$-*b*-$P(PEGMA)_{100}$; $c = 1.0$ mg mL^{-1} at 25 °C.

Critical Micelle Concentration (CMC). The cross-linking process is immediately evident when investigating the surface-active behavior. The block copolymers showed distinctive critical micelle concentrations depending on the macromolecular block sizes. The polymer employed in the cross-linking process $PDMAEMA_{80}$-*b*-P $(PEGMA)_{100}$, showed a sharp drop of surface activity with a CMC of 0.004 mg mL^{-1}. Beyond this concentration, the surface tension remained almost stable at a value of 55 mN m^{-1}. The cross-linking process led to the disappearance of a distinctive CMC value (Figure 10). Similar to earlier results, the surface tension decreased in an almost linear fashion with the logarithm of the polymer concentration. A similar relationship has been observed earlier and is indicative for the enrichment of the polymer along the surface, lowering the free-surface energy similar to that of low molecular weight compounds.[43]

pH Responsiveness. Both the block copolymer and the cross-linked micelles demonstrate a decreasing particle size with increasing pH value with the hydrodynamic diameter suddenly collapsing around pH 7 (Figure 11). As observed earlier in DMAc, the diameter of the micelle tends to decrease upon cross-linking. This effect becomes even more obvious in an aqueous

Table 3. TEM Results of $PDMAEMA_{80}$-*b*-$P(PEGMA)_{100}$ and Its Copolymer Cross-linked by Ethyl Glycol Dimethylacrylate in Aqueous Medium at Different pH Conditions

		diameter (nm) ± 20%	
	concn (mg mL^{-1})	low pH (1−2)	high pH (10−11)
block copolymer	1.0	75	30
cross-linked copolymer	1.0	25	15

environment. The hydrodynamic diameter was observed to be continuously below its uncross-linked counterpart, independent from the pH value (Figure 11). In addition, the volume change with the pH value is restricted upon cross-linking. While a high charge density at low pH value does lead to significant repulsive forces within the core, shell cross-linking prevents considerable swelling of the core.

The sizes of the nanoparticles were investigated using TEM studies, confirming a similar order of magnitude (Table 3).

Stability against Ionic Strength Change. The superior stability of the cross-linked particle becomes more evident when analyzing the micelle size at different ionic strengths. The addition of salt is known to influence the aggregation behavior, and a transition from micelles to vesicles is frequently observed when increasing the ionic strength.[67] A high stability of the aggregated system is particularly important in a physiological environment with a variety of salts, enzymes, and proteins. It is therefore essential for a drug delivery system such as a micelle to remain unaffected by these conditions. Earlier studies revealed that especially high ionic strengths limit the usage of some gene delivery systems.[27] The disintegration at high salt concentration results in the formation of unimers, hence unprotecting sensitive oligonucleotides.

To mimic physiological conditions, the uncross-linked and cross-linked micelles were dissolved in buffer solution to maintain a pH value similar to that of blood (Tris-HCl buffer, pH 7.6). At this pH value (which is close to the pK_a value of DMAEMA), a PDMAEMA block is expected to be partly protonated. The phosphate counterions of DMAEMA, supplied by the buffer, can be replaced by chloride counterions when NaCl is added. The replacement of counterions is known to have dramatic effects on the solubility of polymers or their hydrodynamic diameter.

The diameter of aggregated uncross-linked block copolymer increased gradually from 50 to 100 nm and then suddenly jumped to 250 nm at the highest sodium chloride concentration. This increase in size could be due to electrostatic shielding at high salt concentration. Cross-linked micelles have a strongly contrasting behavior. The cross-linked micelle system remained unaffected by the alteration of the salt concentration. The size of the cross-linked micelles changed only from 25 to 35 nm, indicating excellent stability, even at very high salt concentrations (Figure 12).

(d) Cross-Linked and Uncross-Linked Micelles Based on PDEMAEMA-*b*-P(PEGMA) as Gene Carriers. *Binding of Oligonucleotides: Ethidium Bromide Displacement Assay.* Ethidium bromide is known to easily bind to genes such as a DNA base pair. Gene-bound ethidium bromide exhibits an increased fluorescence.[68] The subsequent addition of cationic polymers is accompanied by a drastic reduction of measured fluorescence derived by the preferential binding between genes and cationic charges.

Experimentally, a gene−ethidium bromide mixture was titrated with cationic polymer, and the fluorescence intensity was recorded (Figure 13). Both, the block copolymer and the

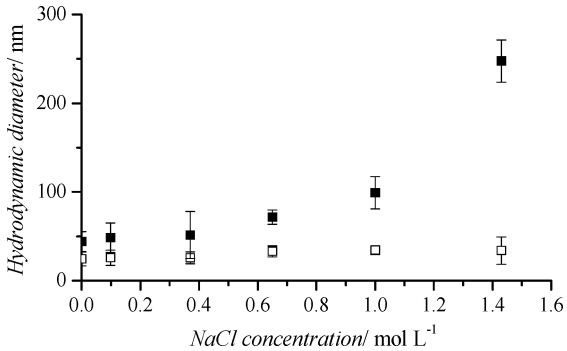

Figure 12. Hydrodynamic diameter of the gene delivery complex (□, cross-linked polymer; ■, uncross-linked polymer) against NaCl concentration in PBS (pH 7.6).

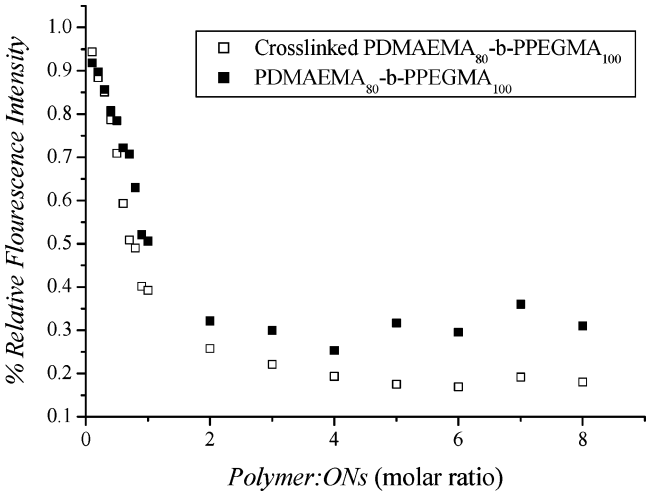

Figure 13. Ethidium bromide displacement by $PDMAEMA_{80}$-*b*-$P(PEGMA)_{100}$ and its cross-linked micelles from Et−Br and gene complexes in PBS (pH 7.6).

cross-linked micelle appear to exhibit good binding properties with oligonucleotides (as suggested by the drop of fluorescence with the addition of cross-linked or uncross-linked copolymer micelles). Fluorescence quenching dropped dramatically from a 0.1 polymer/gene ratio (0.1:1) to a ratio of 2.5 (2.5:1). With increasing polymer concentration, the fluorescence remained approximately stable. For the block copolymer, the lowest relative fluorescence (25.3%) appeared at a molar ratio between polymer and oligonucleotide of 4, and then slightly increased to 35.9% at a ratio of 7. Cross-linked micelles led to an even lower relative fluorescence (16.9%) at a ratio of 6, indicating a slightly better replacement of the ethidium bromide by the polymer.

(e) Cytotoxicity. While the investigations into the transfection efficiency of this possible gene carrier are essential, they cannot be part of this polymerization study. However, it is indispensable to quantify the toxicity of this potential gene carrier. As mentioned earlier, PDMAEMA was shown to have highly toxic properties despite its promising effect as a gene carrier. In addition, it has to be noted that this study employs a dithiobenzoate ester as RAFT agent, which can introduce potential toxicity. A dithiobenzoate RAFT agent, CDB, and polystyrene prepared using CDB were exposed to fibroblast L929 cell lines. While the RAFT agent resulted in cell death of 72%, the resulting polystyrene block copolymer was found to affect less than 10% and can therefore be deemed nontoxic. The incorporation of the RAFT agent into the polymer does therefore reduce its toxicity substantially, probably because of the reduced concentration.

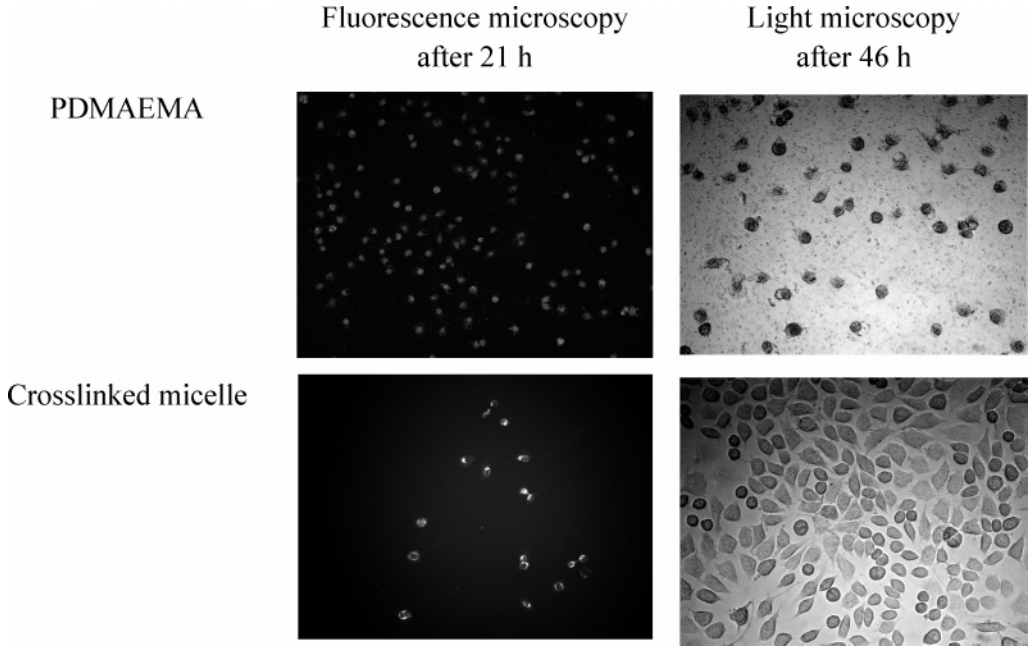

Figure 14. Fluorescence and optical microscope photos of cell line L929 after being exposed to PDMEAMA or the cross-linked micelle for a certain period of time.

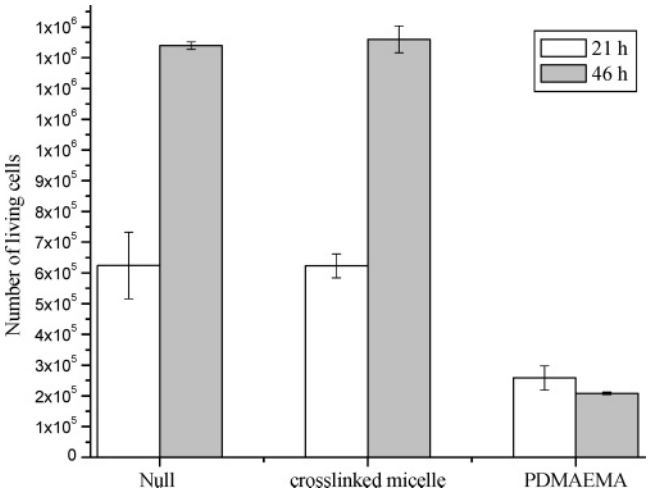

Figure 15. Number of living cells after being exposed to a solution containing PDMEAMA-CDB or the cross-linked micelle ($PDMAEMA_{80}$-*b*-$P(PEGMA)_{100}$) compared to the control experiment without added polymer (Null).

Fluorescence-labeled PDMAEMA prepared using CDB and the final cross-linked micelle were exposed to the same cell lines, and the number of cells was counted after 21 and 46 h, respectively. In addition, the cells were observed using fluorescence and optical microscopy. Fluorescence microscopy was chosen as a suitable tool to confirm the endocytosis of both polymers. It can even be employed to investigate the cellular distribution of nanoparticles to several cytoplasmic organelles.[69] Both fluorescence-labeled polymers were found to enter the cell line after a short period of time as evidenced by the strong fluorescence of these cells (Figure 14). It became very clear, however, after 46 h that the cell lines in the case of linear PDMAEMA did not survive this treatment as evidenced by the round appearance of these cells. In contrast, the L929 maintains its usual appearance after taking up the cross-linked carrier (Figure 14). This observation was quantified by counting the surviving and dead cells. Figure 15 confirms that the cross-linked nanoparticles do not show any signs of toxicity, whereas the linear PDMAEMA clearly limits cell growth.

The cross-linked micelle can therefore be considered nontoxic despite its remaining RAFT end group. By encapsulating the highly toxic PDMAEMA block into a stable and cross-linked PPEGAMA shell, we achieved a significant improvement regarding cytotoxicity.

Conclusions

Cross-linked micelles prepared via further chain extension on the shell from the block copolymers PDMAEMA-*b*-P(PEGMA) have proven to be successfully synthesized by RAFT polymerization. A comparison of NMR, SEC, DLS, TEM, and surface-tension tests between block copolymers and cross-linked micelles provides strong evidence to support the conclusion that the RAFT process is a powerful technique for the stabilization of micellar systems. Alteration of the ionic strength reveals a higher stability of the cross-linked micelles, presenting a delivery system with higher stability. The ethidium bromide displacement assay confirmed the binding ability of the prepared nanoparticles with the cross-linked micelles showing a better binding affinity to ONs. The cross-linked micelles were found to have no toxic effects on the cell line L929, while PDMAEMA strongly inhibited cell growth, leading to substantial cell death. In summary, cross-linked micelle systems were found to be more promising as gene delivery systems compared to classical micellar block copolymer systems.

Acknowledgment. We thank Michael K. C. Tam (Singapore-MIT Alliance, Nanyang Technological University) for helpful discussions. We thank the University of New South Wales and CRC (Cooperative Research Center) for Polymers for a scholarship for L.Z. and L.T.U.N. M.S. acknowledges the ARC (Australian Research Council) for financial support for this project. We also acknowledge the excellent management of the research centre (CAMD) by Dr. Leonie Barner and Mr. Istvan Jacenjik.

Supporting Information Available. The cytotoxicity of cumyl dithiobenzoate (CDB), polystyrene prepared using CDB, PDMAEMA prepared using 4-CAD, and the cross-linked

micelle quantified using cell line L929. This material is available free of charge via the Internet at http://pubs.acs.org.

References and Notes

(1) Ma, D. D. F.; Doan, T. L. *Ann. Intern. Med.* **1994**, *120*, 161−163.
(2) Schreier, H. *Pharm. Acta Helv.* **1994**, *68*, 145−159.
(3) Liu, C. M.; Liu, D. P.; Liang, C. C. *J. Mol. Med.* **2002**, *80*, 620−628.
(4) Frederick, K.; Askari, M. D.; McDonnell, M. *N. Engl. J. Med.* **1996**, 316−319.
(5) Edwin, J.; Sheeja, E.; Pawan, D.; Ajay, T. A.; Viinod, T. *Afr. J. Biotech.* **2004**, *3*, 662−666.
(6) Crooke, S. T.; Leomonidis, K. M.; Neilson, L.; Griffey, R.; Lesnik, E. A.; Monia, B. P. *Biochem. J.* **1995**, *312*, 599−608.
(7) Nielsen, P. E. *Methods Enzymol.* **1999**, *313*, 156−164.
(8) Gryaznov, S.; Chen, J. K. *J. Am. Chem. Soc.* **1994**, *116*, 3141−3144.
(9) Levin, A. A. *Biochem. Biophys. Acta* **1999**, *1489*, 69−84.
(10) Luo, D.; Saltzman, W. M. *Nature Biotechnol.* **2000**, *18*, 33−37.
(11) Park, T. G.; Jeong, J. H.; Kim, S. W. *Adv. Drug Delivery Rev.* **2006**, *58*, 467−486.
(12) Funhoff, A. M.; Monge, S.; Teeuwen, R.; Koning, G. A.; Schuurmans-Nieuwenbroek, N. M. E.; Crommelin, D. J. A.; Haddleton, D. M.; Hennink, W. E.; van Nostruma, C. F. *J. Controlled Release* **2005**, *102*, 711−724.
(13) van de Wetering, P.; Schuurmans-Nieuwenbroek, N. M. E.; van Steenbergen, M. J.; Crommelin, D. J. A.; Hennink, W. E. *J. Controlled Release* **2000**, *64*, 193−203.
(14) van de Wetering, P.; Cherng, J.-Y.; Talsma, H.; Hennink, W. E. *J. Controlled Release* **1997**, *49*, 59−69.
(15) Selva, C.; Gulten, G. *Proceedings of the 8th Polymers for Advanced Technologies International Symposium*, Budapest: Hungary, 2005
(16) Pichot, C.; Elaissari, A.; Duracher, D.; Meunier, F.; Sauzedde, F. *Macromol. Symp.* **2001**, *175*, 285−297.
(17) Rodriguez-Hernandez, J.; Lecommandoux, S. *J. Am. Chem. Soc.* **2005**, *127*, 2026−2027.
(18) Sauer, M.; Streich, D.; Meier, W. *Adv. Mater. (Weinheim, Ger.)* **2001**, 1649−1651.
(19) Sauer, M.; Meier, W. *Chem. Commun.* **2001**, 55−56.
(20) Sauer, M.; Meier, W. *Aust. J. Chem.* **2001**, *54*, 149−151.
(21) Bulmus, V. *Aust. J. Chem.* **2005**, *58*, 411−422.
(22) Lv, H.; Zhang, S.; Wang, B.; Cui, S.; Yan, J. *J. Controlled Release* **2006**, *114*, 100−109.
(23) Li, S.; Ma, Z. *Curr. Gene Ther.* **2001**, *1*, 201−226.
(24) Gref, T.; Luck, M.; Quellec, P.; Marchand, M.; Dellacherie, E.; Harnisch, S.; Blunk, T.; Muller, R. H. *Colloids Surf., B* **2000**, *18*, 301−313.
(25) Pachence, J. M.; Belinka, B.; Simon, P. *Drug Delivery Technol.* **2003**, *3*, 40−45.
(26) Gabizon, A. A. *Clin. Cancer Res.* **2001**, *7*, 223−225.
(27) Rungsardthong, U.; Deshpande, M.; Bailey, L.; Vamvakaki, M.; Armes, S. P.; Garnett, M. C.; Stolnik, S. *J. Controlled Release* **2001**, *73*, 359−380.
(28) Deshpande, M.; Garnett, M. C.; Vamrakaki, M.; Bailey, L.; Armes, S. P.; Stolnik, S. *J. Controlled Release* **2002**, *81*, 185−199.
(29) Tan, J. F.; Ravi, R.; Too, H. P.; Hatoon, T. A.; Tam, K. C. *Biomacromolecules* **2005**, *6*, 498−506.
(30) Ma, Q. G.; Remsen, E. E.; Kowalewski, T.; Schaefer, J.; Wooley, K. L. *Nano Lett.* **2001**, *1*, 651.
(31) Liu, S. Y.; Weaver, J. V. M.; Save, M.; Armes, S. P. *Langmuir* **2002**, *18*, 8350−8357.
(32) Wooley, K. L. *J. Polym. Sci., Part A: Polym. Chem.* **2000**, *38*, 1397−1407.
(33) Iijima, M.; Nagasaki, Y.; Okada, T.; Kato, M.; Kataoka, K. *Macromolecules* **1999**, *32*, 1140−1146.
(34) Emoto, K.; Nagasaki, Y.; Kataoka, K. *Langmuir* **1999**, *15*, 5212−5218.
(35) Won, Y. Y.; Davis, H. T.; Bates, F. S. *Science* **1999**, *283*, 960−963.
(36) Thurmond, K. B.; Kowalewski, T.; Wooley, K. L. *J. Am. Chem. Soc.* **1996**, *118*, 7239−7240.
(37) Huang, H.; Remsen, E. E.; Kowalewski, T.; Wooley, K. L. *J. Am. Chem. Soc.* **1999**, *121*, 3805−3806.
(38) O'Reilly, R. K.; Hawker, C. J.; Wooley, K. L. *Chem. Soc. Rev.* **2006**, *35*, 1068−1083.
(39) O'Reilly, R. K.; Joralemon, M. J.; Hawker, C. J.; Wooley, K. L. *J. Polym. Sci., Part A: Polym. Chem.* **2006**, *44*, 5203−5217.
(40) Barner-Kowollik, C.; Davis, T. P.; Heuts, J. P. A.; Stenzel, M. H.; Vana, P.; Whittaker, M. *J. Polym. Sci., Part A: Polym. Chem.* **2003**, *41*, 365−375.
(41) Perrier, S.; Takolpuckdee, P. *J. Polym. Sci., Part A: Polym. Chem.* **2005**, *43*, 5347−5393.
(42) Moad, G.; Rizzardo, E.; Thang, S. H. *Aust. J. Chem.* **2005**, *58*, 379−410.
(43) Zhang, L.; Katapodi, K.; Davis, T. P.; Barner-Kowollik, C.; Stenzel, M. H. *J. Polym. Sci., Part A: Polym. Chem.* **2006**, *44*, 2177−2194.
(44) Hales, M.; Barner-Kowollik, C.; Davis, T. P.; Stenzel, M. H. *Langmuir* **2004**, *20*, 10809−10817.
(45) Albertin, L.; Stenzel, M. H.; Barner-Kowollik, C.; Foster, L. J. R.; Davis, T. P. *Macromolecules* **2004**, *37*, 7530−7537.
(46) Zheng, G.; Zheng, Q.; Pan, C. *Macromol. Chem. Phys.* **2006**, *207*, 216−223.
(47) Bories-Azeau, X.; Armes, S. P. *Macromolecules* **2002**, *35*, 10241−10243.
(48) (a) Taniguchi, I.; Kuhlman, W. A.; Grifith, L. G.; Mayes, A. M. *Macromol. Rapid Commun.* **2006**, *27*, 631−636. (b) Bo, G.; Wesslen, B.; Wesslen, K. B. *J. Polym. Sci., Part A: Polym. Chem.* **1992**, *30*, 1799.
(49) Wong, K. H.; Davis, T. P.; Barner-Kowollik, C.; Stenzel, M. H. *Polymer*, available on-line June 27, 2007, doi:10.1016/j.polymer.2007.06.048.
(50) Barner, L.; Davis, T. P.; Stenzel, M. H.; Barner-Kowollik, C. *Macromol. Rapid Commun.* **2007**, *28*, 539−559.
(51) Israelachvili, J. N.; Mitchell, D. J.; Ninham, B. W. *J. Chem. Soc., Faraday Trans. 1* **1976**, *72*, 1525−1568.
(52) Förster, S.; Zisenis, M.; Wenz, E.; Antonietti, M. *J. Chem. Phys.* **1996**, *104*, 9956−9970.
(53) Zhu, J.; Lennox, R. B.; Bruce, R.; Eisenberg, A. *Langmuir* **1991**, *7*, 1579−1584.
(54) Ravi, P.; Dai, S.; Tam, K. C.; Gan, L. H. *Langmuir* **2003**, *19*, 5175−5177.
(55) Lee, J. H.; Fetters, L. J.; Archer, L. A. *Macromolecules* **2005**, *38*, 4484−4494.
(56) Noolandi, J.; Hong, K. M. *Macromolecules* **1983**, *16*, 1443−1448.
(57) Halperin, A. *Macromolecules* **1987**, *20*, 2943−2946.
(58) Garnier, S.; Laschewsky, A. *Colloid Polym. Sci.* **2006**, *284*, 1243−1254.
(59) Colby, R. H.; Plucktaveesak, N.; Bromber, L. *Langmuir* **2001**, *17*, 2937−2941.
(60) Couderc-Azouani, S.; Sidhu, J.; Georgiou, T. K.; Charahambous, D. C.; Vamvakaki, M.; Patrickios, C. S.; Bloor, D. M.; Penfold, J.; Holzwarth, J. F.; Wyn-Jones, E. *Langmuir* **2004**, *20*, 6458−6469.
(61) Spevacek, J. *Macromol. Chem. Rapid Commun.* **1982**, *3*, 697−703.
(62) Ni, P. H.; Pan, Q. S.; Zha, L. S.; Wang, C. C.; Elaissari, A.; Fu, S. K. *J. Polym. Sci., Part A: Polym. Chem.* **2002**, *40*, 624−631.
(63) Lowe, A. B.; Billingham, N. C.; Armes, S. P. *Macromolecules* **1998**, *31*, 5991−5998.
(64) Vamvakaki, M.; Billingham, N. C.; Armes, S. P. *Macromolecules* **1999**, *32*, 2088−2090.
(65) Gao, Z.; Zhong, X. F.; Eisenberg, A. *Macromolecules* **1994**, *27*, 794−802.
(66) Yang, L. − P.; Pan, C. − Y. *Aust. J. Chem.* **2006**, *59*, 733−736.
(67) Soo, P. L.; Eisenberg, A. *J. Polym. Sci., Part B: Polym. Phys.* **2004**, *42*, 923−938.
(68) Wiethoff, C. M.; Gill, M. L.; Loe, G. S.; Koe, J. G.; Middaugh, C. R. *J. Pharm. Sci.* **2003**, *92*, 1272−1285.
(69) Savic, R.; Luo, L.; Eisenberg, A.; Maysinger, D. *Science* **2004**, *303*, 627−628.

BM070370G